أكاديمية كاوست
KAUST ACADEMY

جامعة الملك عبدالله
للعلوم والتقنية
King Abdullah University of
Science and Technology

Fog to Water: Harvesting the Invisible through Kirigami Design and Surface Engineering

Moawiah Safwan Bourgleh
Supervisor: Prof. Qiaoqiang Gan
Mentor: Dr. Shakeel Ahmed

moawiahsm@gmail.com
qiaoqiang.gan@kaust.edu.sa
shakeel.ahmad@kaust.edu.sa

Abstract

Saudi Arabia faces continuing pressure on its water supply because of its dry climate, low rainfall, and limited natural freshwater resources. At the same time, frequent fog in the southwestern highlands offers a local source of suspended water droplets that can be collected without active cooling or vapour condensation. This project examined how collector geometry and surface condition affect passive fog-water collection and aimed to identify the best-performing combination under controlled laboratory conditions. Four uncoated designs were compared: a kirigami collector with internal drainage channels, a Fog Harp, a fine metal mesh, and a double-layer Raschel mesh. Selected collectors were also tested with a superhydrophobic coating and a lubricated surface, together with a hybrid Fog Harp–kirigami arrangement. Performance was evaluated using the area-normalized water collection rate. Among the uncoated designs, kirigami achieved the highest rate at 2.576 $\mathrm{L\,m^{-2}\,h^{-1}}$. With a lubricated surface, the rates increased to 4.703 $\mathrm{L\,m^{-2}\,h^{-1}}$ for kirigami and 3.924 $\mathrm{L\,m^{-2}\,h^{-1}}$ for the Fog Harp. The lubricated hybrid arrangement produced the highest rate in the study at 5.488 $\mathrm{L\,m^{-2}\,h^{-1}}$. These results show that fog collection depends on both droplet interception and water drainage. Collector geometry and surface condition should therefore be designed together as parts of one collection system.

Date: August 15, 2026

Contents

List of Tables 2

List of Figures 3

1 Introduction 4

2 Related Work 6

3 Materials and Methods 10

3.1 Method Details . . . 10

3.2 Evaluation Procedure . . . 13

4 Results 13

4.1 Effect of Collector Geometry . . . 14

4.2 Effect of Surface Condition . . . 15

4.3 Performance of the Hybrid Collector . . . 15

4.4 Overall Performance Comparison . . . 16

5 Discussion 16

5.1 Effect of Collector Geometry . . . 16

5.2 Effect of Surface Condition . . . 17

5.3 Performance of the Hybrid Collector . . . 18

6 Limitations and Future Work 20

6.1 Limitations . . . 20

6.2 Future Work . . . 20

7 Conclusion 21

References 21

List of Tables

1 Comparison of geometry-based passive fog collectors. 8

2 Collector dimensions and projected areas used for normalization. 11

3 Experimental test matrix. 12

4 Area-normalized water collection rates for all tested conditions. 14

5 Main performance comparisons. 19

List of Figures

1 Average annual rainfall across Saudi Arabia. . . . 4
2 Formation of orographic fog in southwestern Saudi Arabia. . . . 5
3 Main stages of passive fog-water harvesting. . . . 5
4 Main limitations of conventional crossed-fibre fog-collection meshes. . . . 7
5 Comparison of geometry-based passive fog-water collectors. . . . 8
6 Qualitative effects of surface treatment on fog-droplet behaviour. . . . 9
7 Experimental fog-collection system. . . . 11
8 Collectors used in the baseline geometry comparison. . . . 12
9 Collection rates of the uncoated collector geometries. . . . 14
10 Collection rates under the tested surface conditions. . . . 15
11 Collection rates of configurations with lubricated surfaces. . . . 16
12 Proposed collection mechanisms of the kirigami geometry. . . . 17
13 Droplet behaviour under the tested surface conditions. . . . 18
14 Hybrid Fog Harp–kirigami configuration. . . . 19

1 Introduction

Saudi Arabia faces a major challenge in securing enough water because of its dry climate, low rainfall, and limited natural freshwater resources. The country covers about 2.25 million km^2 but has no permanent rivers. Its average annual rainfall is around 100–150 mm, with large differences between regions, as shown in Figure 1. Surface water is therefore mainly available as short-term runoff through valleys after rainfall, rather than as a continuous water supply [1]. For this reason, Saudi Arabia depends heavily on seawater desalination, groundwater extraction, and treated wastewater reuse. These sources are essential, but they require energy and can have economic and environmental costs [3]. It is therefore useful to study other water sources that could support the existing supply in suitable locations.

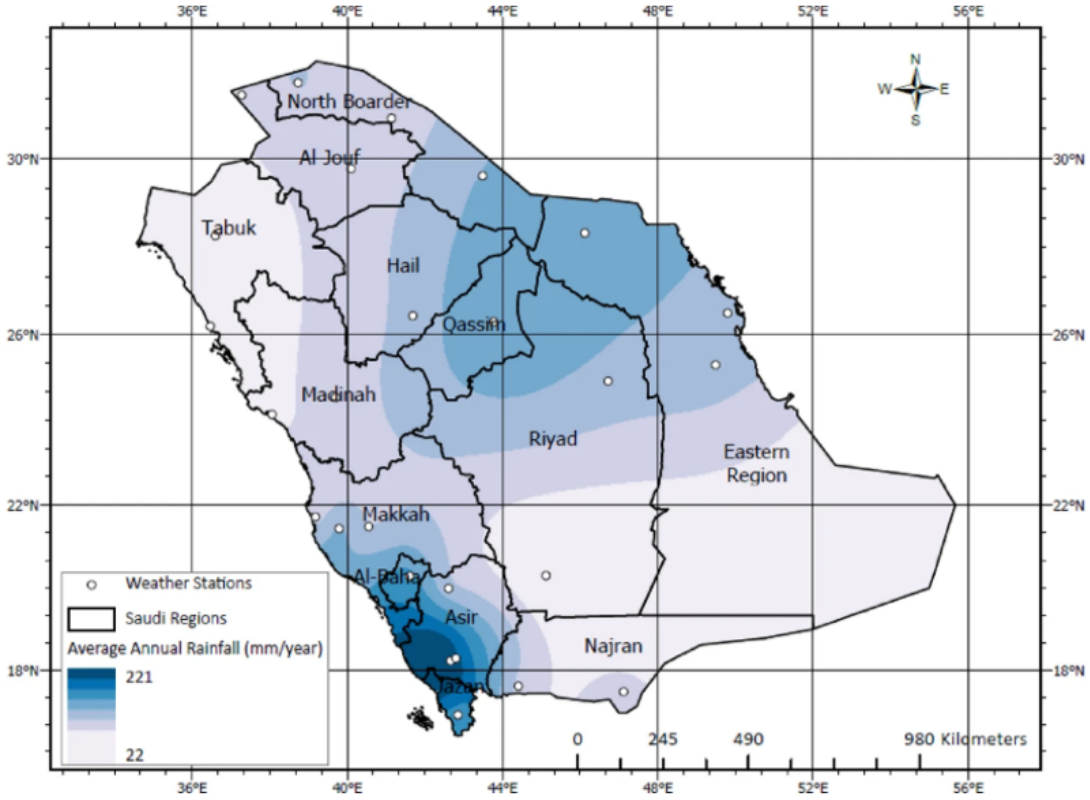


Figure 1 Average annual rainfall across Saudi Arabia. The southwestern regions, including Asir, Al-Baha, and Jazan, receive more rainfall than most central and northern parts of the country. Adapted from Fig. 12 in *Fog Harvesting Implementation as a Sustainable Water Source: A Feasibility Study in Al-Baha, Saudi Arabia* [2].

Fog is a possible source of water in the mountainous areas of southwestern Saudi Arabia [2]. It can be described as a cloud that forms near the ground and contains very small water droplets suspended in the air [5, 6]. In mountain regions, orographic fog forms when moist air moves toward a mountain and rises along its slopes. As the air rises, it becomes cooler. When it reaches the dew-point temperature, the water vapour begins to condense into small liquid droplets, forming fog or low clouds. This process helps explain why fog often appears in the southwestern highlands. Field studies in Al-Soudah and Al-Baha have shown that the local conditions may be suitable for fog-water harvesting, especially during seasons when fog occurs frequently [4, 2].

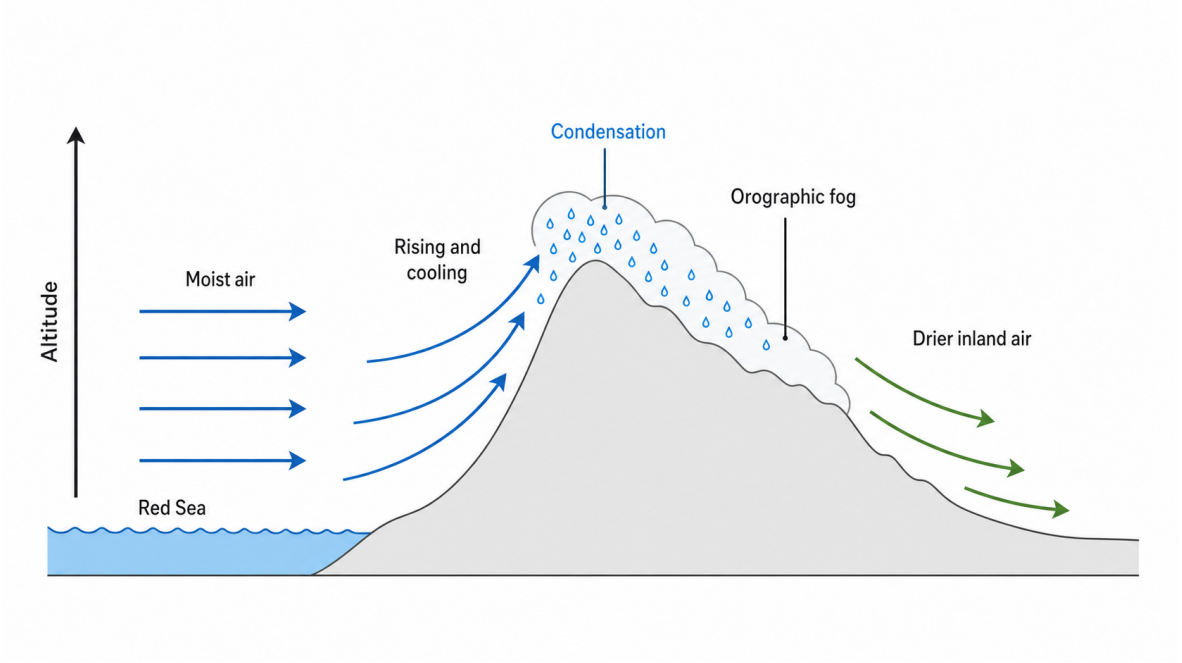


Figure 2 Formation of orographic fog in southwestern Saudi Arabia. Moist air rises along a mountain slope, cools to its dew point, and condenses into small water droplets. A fog collector can be placed on an exposed mountain ridge where fog-laden air passes through it. Original illustration created for this report.

Fog harvesting is different from collecting water vapour from humid air. Fog already contains liquid droplets, so a passive fog collector does not need to cool the air or condense the water vapour. A collector is usually placed vertically and approximately perpendicular to the fog-laden airflow. When the air passes through it, some fog droplets hit its surface and remain attached. The small droplets then join together to form larger droplets through a process called coalescence. As the droplets grow, their weight increases. Once gravity becomes stronger than the force holding them to the surface, they move downward into a collection channel and then into a storage container [7, 8]. The process can therefore be divided into three main stages: droplet interception, coalescence, and drainage.

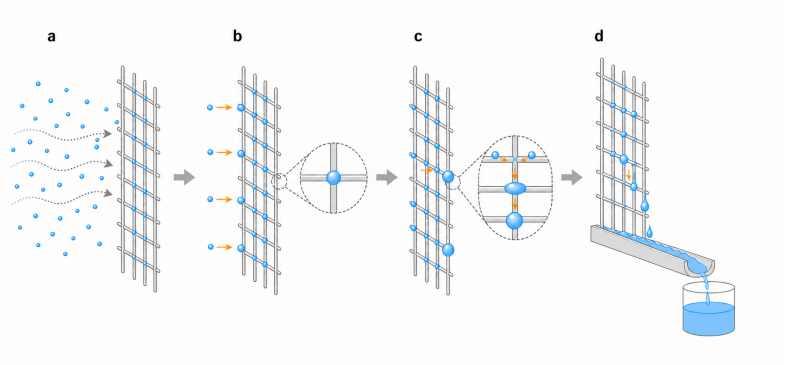


Figure 3 Main stages of passive fog-water harvesting: (a) fog droplets are intercepted by the collector, (b) small droplets join to form larger droplets, and (c) the collected water drains into a channel and storage container. Original illustration created for this report.

However, the presence of fog does not always lead to efficient water collection. The main engineering problem is to design a collector that captures a large number of droplets without blocking the airflow and that allows the collected water to drain quickly. If the openings are too large, many fog droplets may pass through without touching the collector. If the openings are too small, the collector may restrict the airflow, especially when water builds up and partly blocks them [9, 10]. Water may also remain trapped on horizontal parts or at mesh intersections. In other cases, captured droplets may be carried away by the airflow before they reach the collection channel [8]. The geometry and surface properties of a collector must therefore be studied together.

This study compared four passive fog collectors: a kirigami collector with small internal drainage channels, a Fog Harp, a fine metal mesh, and a double-layer Raschel mesh. The uncoated designs provide a baseline for comparing collector geometry. Selected collectors were then tested with a superhydrophobic coating and a lubricated surface, and a hybrid Fog Harp–kirigami arrangement was also evaluated. All configurations were tested using the same laboratory system. The study measures the liquid delivered to the collection tray and reports the area-normalized water collection rate. Its aim is to determine how collector geometry and surface condition work together and to identify the best-performing configuration under the laboratory conditions used.

2 Related Work

Most conventional fog-harvesting applications use mesh collectors installed vertically and approximately perpendicular to fog-laden winds. These collectors are commonly made from polymeric mesh, such as Raschel mesh, or from metal mesh mounted within a frame. Their use has become widespread because they are simple, relatively inexpensive to produce, and can be scaled up to collect larger volumes of water in locations where fog occurs frequently [13, 14]. When air passes through the mesh, some fog droplets collide with the fibres and remain attached to them. These droplets then coalesce to form larger droplets that move downward under gravity. However, a mesh cannot capture all the droplets in its path. Part of the airflow may be diverted around the collector, while some droplets pass through the openings or follow the airflow streamlines around the fibres without colliding with them [14]. Water may also accumulate between intersecting fibres, partially blocking the openings and restricting airflow. In addition, droplets may remain trapped at fibre intersections or become re-entrained in the airflow before reaching the collection channel [9, 10]. These four limitations are illustrated in Figure 4. Therefore, conventional meshes provide a practical solution and a useful benchmark for comparing alternative designs, but their intersecting structure may limit water drainage and airflow through the collector.

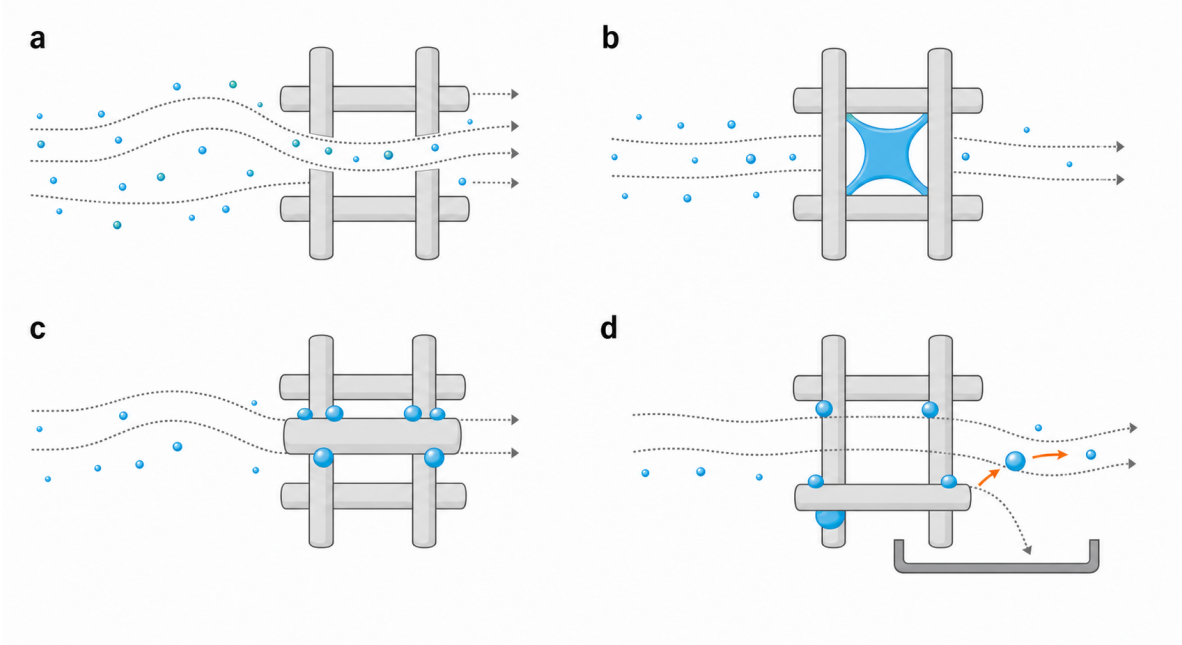


Figure 4 Main limitations of conventional crossed-fibre fog-collection meshes: (a) some fog droplets follow the airflow through the openings without colliding with the fibres; (b) accumulated water may bridge the openings and restrict airflow; (c) droplets may remain pinned to horizontal fibres and intersection points instead of draining; and (d) captured droplets may become re-entrained in the airflow before reaching the collection channel. Original illustration created for this report based on the mechanisms discussed in [9, 10, 14]; not to scale.

The limitations of intersecting mesh networks have led researchers to change collector geometry rather than focus only on material selection. One prominent example is the Fog Harp, which replaces crossed horizontal and vertical fibres with parallel vertical wires. The design can be described as an array of one-dimensional elements arranged within a two-dimensional frame. Its vertical wires provide direct drainage paths, which reduce water retention at intersections and help prevent the openings from becoming blocked. In controlled laboratory experiments, Shi et al. reported a water-collection rate approximately three times that of an equivalent mesh tested under the same conditions [10]. A later one-year field study showed that a full-scale Fog Harp could collect water during light-fog events in which the conventional mesh used for comparison produced no measurable collection [15]. However, scaling up the design introduces another challenge: wet wires may move closer together or stick because of capillary forces. Fog-Harp performance therefore also depends on wire length, tension, spacing, and the method used to attach the wires to the frame [17].

Kirigami collectors use a different geometric approach. Cuts and folds transform a flat sheet into a three-dimensional structure. Li et al. showed that these folds can change the airflow around the collector and generate vortices that redirect some fog droplets toward its surfaces. The folded geometry can also guide the collected water toward drainage points [11]. Bintein et al. later studied a different kirigami net made from interconnected strips. Stable water films formed on the strips, allowing collection and drainage to continue without closing the open flow passages [16]. Under the artificial-fog conditions used in that study, the strip-based design began draining sooner and achieved a higher collection efficiency than the conventional fibre nets tested in the same apparatus. Together, these studies show that collector geometry affects both droplet interception and water drainage. However, they do not establish one design as universally superior because performance also depends on collector dimensions, element tension, air velocity,

fog properties, and the test method. Table 1 summarizes the main geometric approaches, while Figure 5 illustrates their different collection and drainage mechanisms.

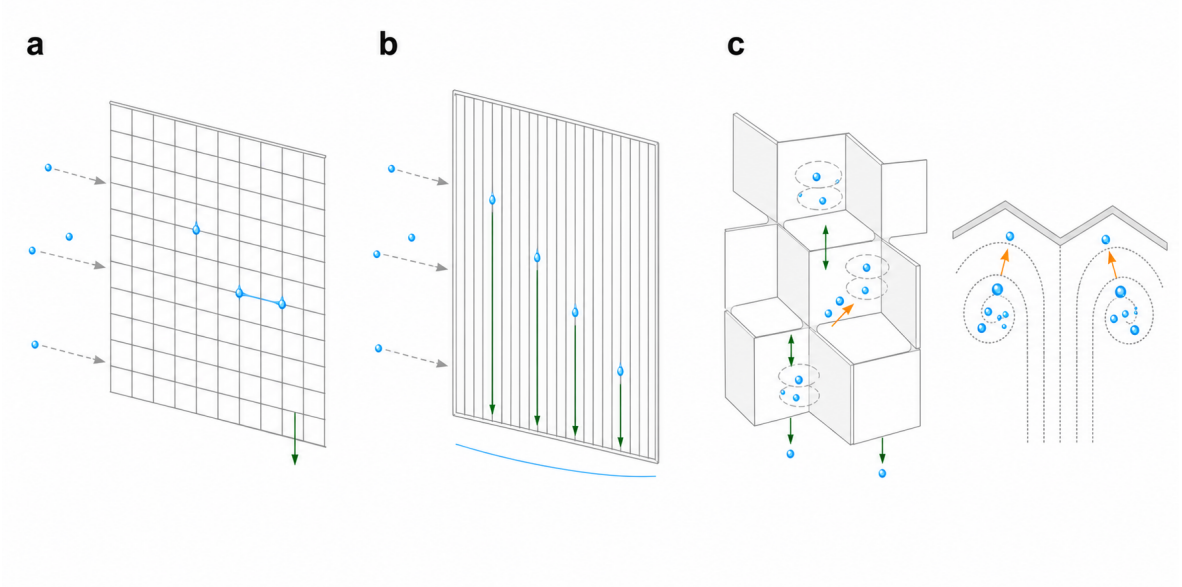


Figure 5 Conceptual comparison of geometry-based passive fog-water collectors. (a) A conventional crossed mesh can retain droplets at fibre intersections and form water bridges. (b) A Fog Harp provides vertical, intersection-free drainage paths. (c) A three-dimensional kirigami collector modifies the local airflow and guides intercepted water downward. Grey arrows indicate fog-laden airflow, while green arrows indicate gravity-driven drainage. Original illustration created for this report; not to scale.

Table 1 Comparison of geometry-based passive fog collectors. Reported performance values are not directly comparable because the cited studies used different fog and airflow conditions.

Collector	Geometric principle	Main advantage	Reported limitation
Crossed mesh [9, 10, 14]	Intersecting horizontal and vertical fibres	Simple, inexpensive, and scalable	Water may be pinned at intersections, bridge openings, and restrict airflow
Fog Harp [10, 15, 17]	Fine parallel vertical wires	Direct drainage with no intersections in the active area	Long wet wires may tangle; performance depends on tension and attachment
Three-dimensional kirigami [11]	Cut-and-folded units that reshape the local airflow	Vortices can redirect droplets, while folds guide drainage	Performance depends on fold geometry, orientation, and airflow conditions
Strip-based kirigami [16]	Interconnected strips that support a continuous water film	Open flow passages are maintained while water drains along the strips	Evidence was obtained under artificial-fog conditions that differ from natural fog

The surface properties of a collector affect how fog droplets attach, move, and drain after hitting the surface. On hydrophilic surfaces, the droplets spread and may form a continuous water film. However, some water may remain attached to the surface, which delays its movement towards the collection channel. Hydrophobic surfaces usually form separate droplets with smaller contact areas, allowing them to move and detach more easily. However, stronger water repellency does not always increase the amount of water that reaches the collection tray. On highly water-repellent surfaces, droplets may bounce or detach in the wrong direction and miss the collection path [11]. Seo et al. compared hydrophilic, hydrophobic, superhydrophobic, and oil-infused surfaces, including surfaces treated with silicone oils of different viscosities. Their results showed that water removal was an important part of fog collection. Under their test conditions, the oil-infused surfaces achieved the best performance because they offered less resistance to droplet movement [12]. However, the oil layer may be gradually lost during operation, which can reduce its slippery properties over time [18]. Therefore, this study tests a superhydrophobic coating and a lubricated surface condition as two different methods of controlling droplet movement and drainage. It does not assume that either treatment will be the best for every collector design or operating condition. Figure 6 shows the expected droplet behaviour under these surface conditions.

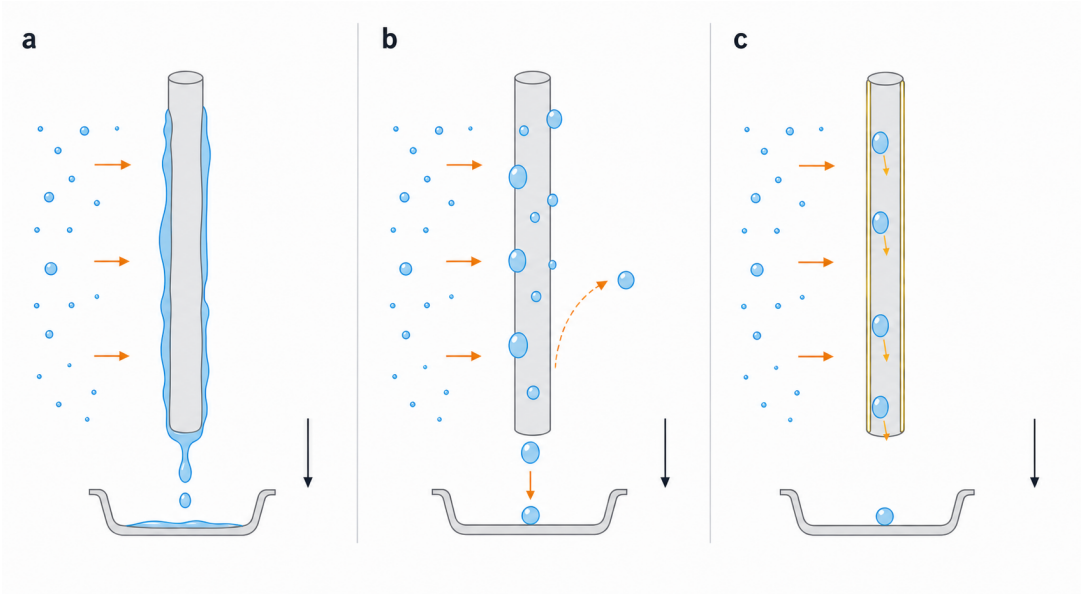


Figure 6 Qualitative effects of surface treatment on fog-droplet behaviour. (a) On an uncoated surface, water may spread along the collector element and remain attached before draining. (b) A collector treated with a superhydrophobic coating promotes the formation of more separate droplets and may allow easier shedding, although some droplets may rebound from the surface. (c) A lubricated surface may reduce resistance to droplet movement and support downward sliding. The figure does not present a quantitative performance ranking because the result also depends on collector geometry and the test conditions. Original illustration created for this report.

Although previous studies have examined fog-collector geometry and surface properties, their results do not give a fixed ranking that applies under all conditions. Some studies compared different collector designs while keeping the surface treatment constant [11]. Other studies showed that mesh performance is affected by air speed, the liquid-water content of the fog, droplet size, and test duration [19, 20]. This project examines the relationship between collector geometry and surface condition by measuring the mass of liquid that reaches the collection tray and reporting the area-normalized water collection rate. Four uncoated collectors were studied: the kirigami collector with internal channels, the Fog Harp, the fine metal mesh, and

the double-layer Raschel mesh. The superhydrophobic coating was also tested on the kirigami collector, the Fog Harp, and the fine metal mesh. A lubricated surface condition was then tested on the kirigami collector, the Fog Harp, and a combined arrangement in which the Fog Harp was placed in front of the kirigami collector. These comparisons aim to identify the collector configuration and surface condition that produced the highest collection rate under the laboratory conditions used. They also help explain how collector geometry and surface treatment work together to capture fog droplets and drain the collected liquid into the tray.

3 Materials and Methods

This section describes the laboratory fog-collection system, the collector geometries, the applied surface conditions, and the procedure used to quantify the water delivered to the collection tray. All tests were performed using the same apparatus and nominal operating settings. The measured mass was normalized by the projected frontal area of each collector and the nominal evaluation time.

3.1 Method Details

3.1.1 Experimental Fog-Collection System

The experiments were conducted in a KAUST laboratory using a small enclosed fog chamber placed inside a fume hood. The approximately box-shaped chamber was constructed mainly from insulating foam boards and included a transparent viewing panel. Fog was generated using a commercial ultrasonic humidifier filled with tap water. The humidifier was operated at a fixed output setting during the tests. A separate one-hour weighing check indicated an approximate humidifier-assembly mass loss of 146 $g\,h^{-1}$, which was used only as an operating reference.

A computer fan transported the air–fog mixture through a transparent delivery tube toward the collector. A nominal air speed of approximately 2.6 $m\,s^{-1}$ was maintained during the tests. The final tube section had an approximate diameter of 7 cm and was inclined downward toward the collector by about 15°. The outlet was positioned approximately 5 cm from the collector.

Each collector was mounted approximately vertically in an acrylic frame, with its frontal plane approximately perpendicular to the incoming fog-laden airflow. A transparent plastic tray was positioned directly below the collector to receive the drained water. Figure 7 shows the main components of the experimental system.

3.1.2 Collector Designs and Dimensions

Five collector configurations were tested: a kirigami collector, a Fog Harp, a fine metal mesh, a double-layer Raschel mesh, and a combined Fog Harp–kirigami configuration. The projected area used for normalization was the complete active rectangular frontal footprint, including the openings and excluding the supporting frame.

The kirigami collector was fabricated from a thin, transparent laser-cut polymer sheet. It contained repeated triangular units with laser-cut openings and engraved surface channels. Each triangular unit had an approximate outer side length of 1.5 cm, and the three-dimensional structure had an approximate fold angle of 120°. During testing, the concave side containing the engraved channels faced the incoming fog.

The Fog Harp consisted of approximately vertical parallel metal wires mounted in an acrylic frame. The recorded wire diameter and spacing were approximately 0.5 mm and 2 mm, respectively, while the active wire length was approximately 10 cm. The fine metal mesh consisted of a single crossed-wire layer mounted in a similar frame. The double-layer Raschel collector

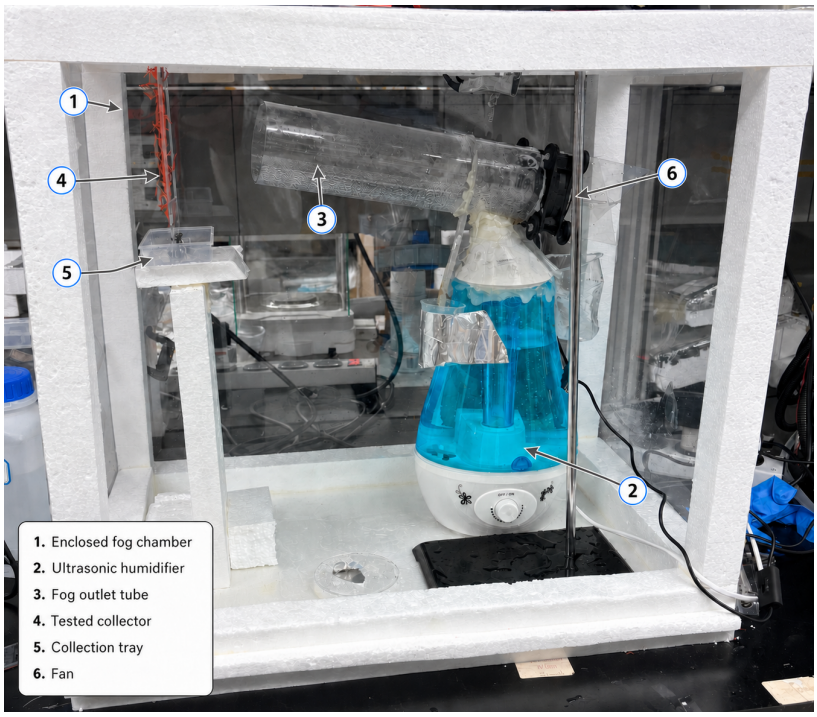


Figure 7 Experimental fog-collection system showing the enclosed chamber, ultrasonic humidifier, fog-delivery tube, tested collector, collection tray, and computer fan. Photograph taken during this study.

contained two orange mesh layers placed in direct or near-direct contact.

For the combined configuration, the Fog Harp was positioned in front of and directly adjacent to the kirigami collector. The incoming fog passed through the harp before reaching the overlapping part of the kirigami, and both collectors drained toward the same tray. An 80 cm^2 projected footprint, corresponding to the frontal area of the larger kirigami collector, was used for normalization.

Table 2 Active projected dimensions and areas used for normalization.

Collector	Condition	Width (cm)	Height (cm)	Area (cm^2)
Kirigami	Uncoated	2.5	10	25
Kirigami	Superhydrophobic coating	8	10	80
Kirigami	Lubricated surface	8	10	80
Fog Harp	Uncoated	5	10	50
Fog Harp	Superhydrophobic coating	5.5	10	55
Fog Harp	Lubricated surface	5.5	10	55
Fine metal mesh	Uncoated	4.4	10	44
Fine metal mesh	Superhydrophobic coating	8	10	80
Double-layer Raschel	Uncoated	7.5	10	75
Harp–kirigami	Lubricated surface	8	10	80[a]

[a]The projected area was based on the frontal footprint of the larger kirigami collector. Projected area includes the openings within the active footprint and excludes the supporting frame.

The four baseline collector geometries are shown in Figure 8.

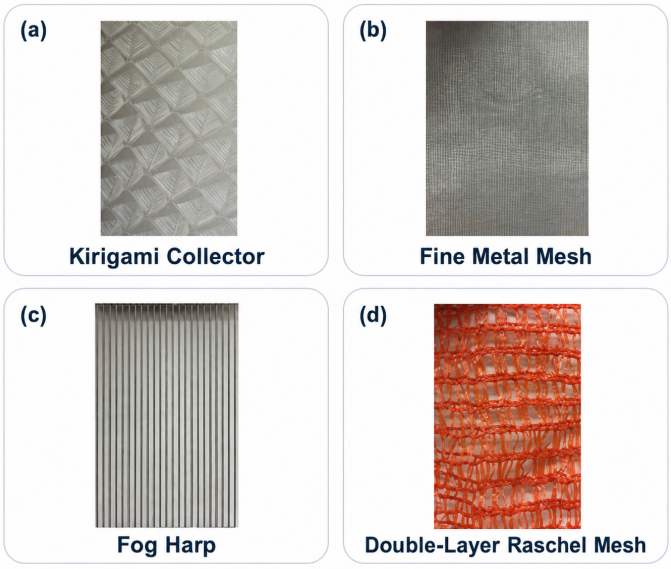


Figure 8 Fog collectors evaluated in the baseline geometry comparison: (a) kirigami collector with repeated folded triangular units, (b) fine crossed metal mesh, (c) Fog Harp with parallel vertical wires, and (d) double-layer Raschel mesh. Source photographs taken during this study; composite prepared for this report.

3.1.3 Surface Preparation and Treatments

Uncoated collectors were tested without an intentionally applied surface treatment. For the coated conditions, a commercial-grade superhydrophobic coating was sprayed on both sides of each selected collector. Two coating layers were applied, with approximately one hour of drying after each layer. Visible droplet beading was observed after treatment. The term *superhydrophobic coating* is used throughout this report as the treatment label; quantitative surface characterization is addressed in the study limitations.

For the lubricated surface condition, the coating was renewed using one additional spray layer before a commercial-grade lubricant with a nominal kinematic viscosity of 10 cSt was applied to both sides. Each sample was then shaken manually for approximately two minutes to remove excess lubricant.

3.1.4 Experimental Test Matrix

Table 3 summarizes the tested combinations of collector geometry and surface condition.

Table 3 Experimental test matrix.

Collector configuration	Uncoated	Superhydrophobic coating	Lubricated surface
Kirigami	Tested	Tested	Tested
Fog Harp	Tested	Tested	Tested
Fine metal mesh	Tested	Tested	–
Double-layer Raschel mesh	Tested	–	–
Fog Harp–kirigami combination	–	–	Tested

The lubricated surface conditions used a renewed superhydrophobic coating. In the combined

configuration, the Fog Harp was positioned in front of the kirigami collector.

3.2 Evaluation Procedure

3.2.1 Experimental Procedure

Before each test, the collection-tray assembly was emptied and weighed without the collector. The weighed assembly included the transparent tray, its permanently attached clip, and the fixing silicone. The same balance was used throughout the tests, with a display resolution of 0.01 g.

The collector was mounted vertically above the tray and positioned approximately perpendicular to the fog-laden flow. For the kirigami samples, the concave channel-containing side faced the incoming fog. The system was operated for a six-minute stabilization period with the collector and tray installed. This was followed by a nominal 30-minute evaluation period. The superhydrophobic-coated Fog Harp was evaluated for 60 minutes.

At the end of each test, the system was stopped and the collector frame was removed. Water remaining on the collector was not manually transferred to the tray. The tray assembly was weighed outside the chamber, and the initial and final balance readings were recorded photographically.

3.2.2 Mass Measurement and Rate Calculation

The collected water mass was calculated from the increase in tray-assembly mass:

$$\Delta m = m_f - m_i, \tag{1}$$

where m_i and m_f are the initial and final tray-assembly masses in grams, respectively.

The area-normalized water collection rate was calculated using one general equation for all collector configurations and surface conditions:

$$R_{\text{collected}} = \frac{\Delta m}{1000 A t} = \frac{m_f - m_i}{1000 A t}, \tag{2}$$

where $R_{\text{collected}}$ is expressed in $\mathrm{L\,m^{-2}\,h^{-1}}$, A is the projected frontal area in $\mathrm{m^2}$, and t is the nominal evaluation time in hours. The factor 1000 converts the measured mass in grams to a water-volume equivalent using a water density of $1\ \mathrm{kg\,L^{-1}}$.

For example, the uncoated kirigami test had $m_i = 20.82$ g, $m_f = 24.04$ g, $A = 0.0025\ \mathrm{m^2}$, and $t = 0.5$ h. Therefore, $\Delta m = 3.22$ g and $R_{\text{collected}} = 2.576\ \mathrm{L\,m^{-2}\,h^{-1}}$.

3.2.3 Measurement Scope

The primary measurement was the increase in collection-tray mass. This value represented water that reached the tray after the combined processes of droplet interception, coalescence, and drainage. Water remaining on the collector was not included in the measured output. The experimental boundaries and their effects on interpretation are discussed in the Limitations section.

4 Results

This section compares the ten tested combinations of collector geometry and surface condition. Performance is reported as the area-normalized water collection rate in $\mathrm{L\,m^{-2}\,h^{-1}}$. This measure normalizes the collected mass by projected collector area and test duration. Table 4 lists the measured rate for every tested condition.

Table 4 Area-normalized water collection rates for all tested collector configurations and surface conditions.

Collector configuration	Surface condition	Rate ($L\,m^{-2}\,h^{-1}$)
Double-layer Raschel mesh	Uncoated	1.501
Fine metal mesh	Uncoated	1.764
Fine metal mesh	Superhydrophobic coating	1.920
Fog Harp	Uncoated	2.032
Fog Harp	Superhydrophobic coating	2.233
Kirigami	Uncoated	2.576
Kirigami	Superhydrophobic coating	3.825
Fog Harp	Lubricated surface	3.924
Kirigami	Lubricated surface	4.703
Fog Harp–kirigami	Lubricated surface	5.488

4.1 Effect of Collector Geometry

The four uncoated collectors were compared first to examine the effect of geometry without an intentionally applied surface treatment. As shown in Figure 9, the kirigami collector recorded the highest rate at 2.576 $L\,m^{-2}\,h^{-1}$. The Fog Harp ranked second at 2.032 $L\,m^{-2}\,h^{-1}$, followed by the fine metal mesh at 1.764 $L\,m^{-2}\,h^{-1}$. The double-layer Raschel mesh recorded the lowest rate at 1.501 $L\,m^{-2}\,h^{-1}$.

Using the Raschel mesh as the baseline, the measured rate was 71.6% higher for the kirigami collector, 35.4% higher for the Fog Harp, and 17.5% higher for the fine metal mesh. The kirigami collector was therefore the best-performing uncoated geometry under the laboratory conditions used in this study.

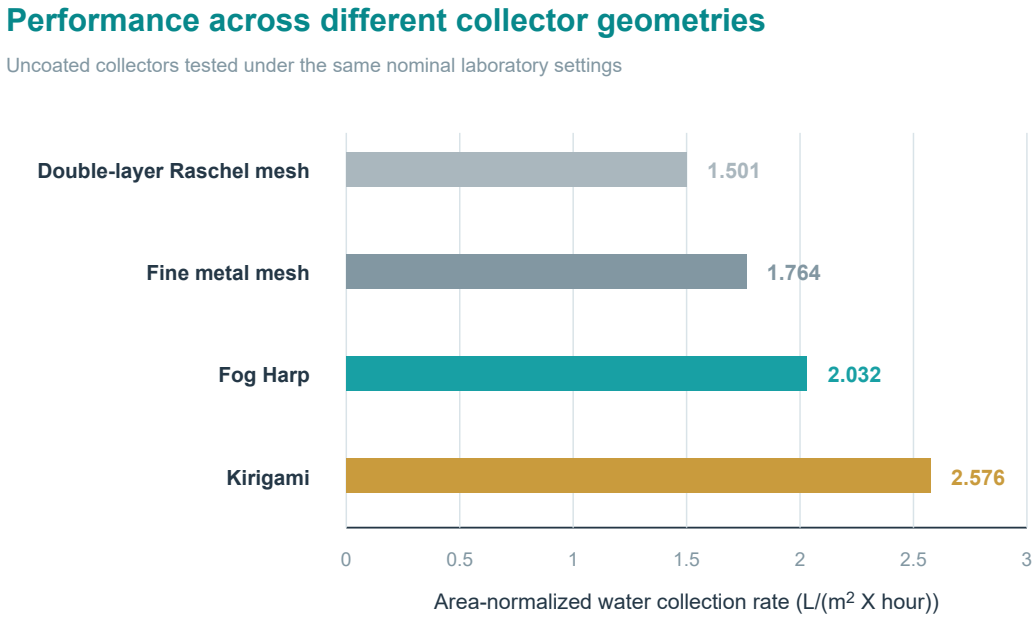


Figure 9 Area-normalized water collection rates of the four uncoated collector geometries. Exact measured values are shown at the ends of the bars.

4.2 Effect of Surface Condition

Figure 10 compares the measured rates across the available surface conditions. Some collector dimensions differed between conditions; therefore, the normalized rates describe the tested condition as a whole rather than the isolated effect of the surface treatment. For the kirigami collector, the superhydrophobic-coated condition recorded 3.825 $L\,m^{-2}\,h^{-1}$, which was 48.5% higher than the uncoated result of 2.576 $L\,m^{-2}\,h^{-1}$. The superhydrophobic-coated Fog Harp recorded 2.233 $L\,m^{-2}\,h^{-1}$, which was 9.9% above its uncoated result. The superhydrophobic-coated fine metal mesh recorded 1.920 $L\,m^{-2}\,h^{-1}$, which was 8.8% above its uncoated result of 1.764 $L\,m^{-2}\,h^{-1}$.

The lubricated condition recorded the highest measured rate for both collector designs tested in all three surface conditions. The kirigami collector with a lubricated surface recorded 4.703 $L\,m^{-2}\,h^{-1}$. This value was 23.0% above the superhydrophobic-coated kirigami and 82.6% above the uncoated kirigami. The Fog Harp with a lubricated surface recorded 3.924 $L\,m^{-2}\,h^{-1}$, which was 75.7% above its superhydrophobic-coated condition and 93.1% above its uncoated condition.

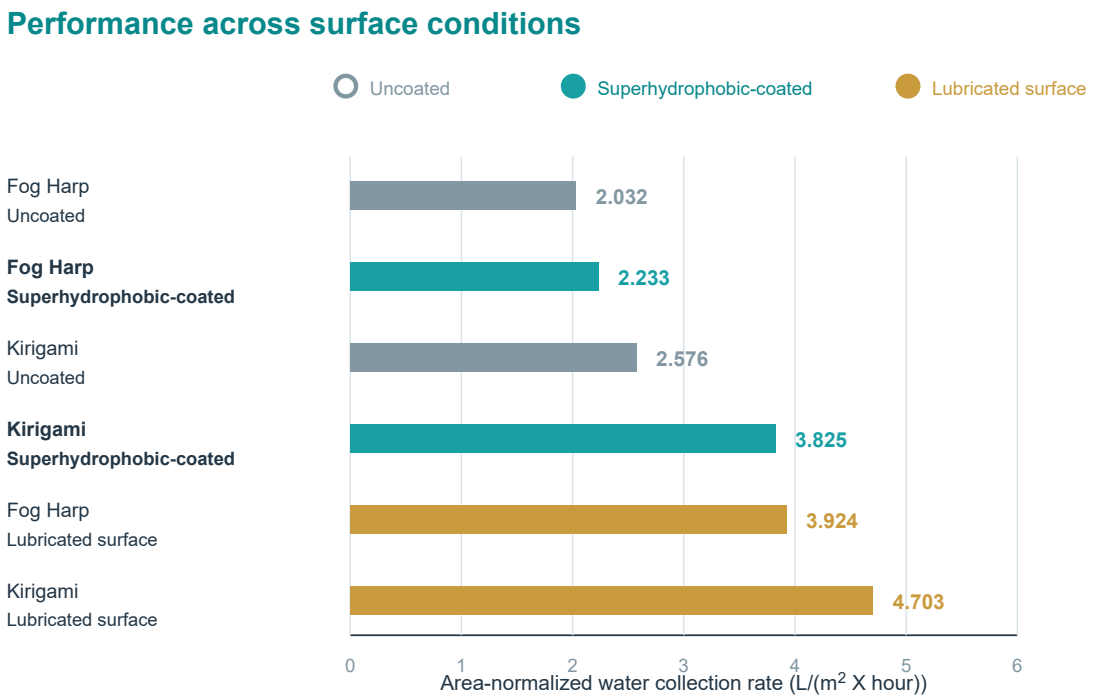


Figure 10 Comparison of the area-normalized water collection rate across the tested surface conditions. Exact values are shown at the ends of the bars. A lubricated surface condition was not tested for the fine metal mesh.

4.3 Performance of the Hybrid Collector

The Fog Harp–kirigami configuration with lubricated surfaces recorded a rate of 5.488 $L\,m^{-2}\,h^{-1}$, the highest value measured in this study. As shown in Figure 11, this rate was 16.7% higher than the kirigami with a lubricated surface and 39.9% higher than the Fog Harp with a lubricated surface.

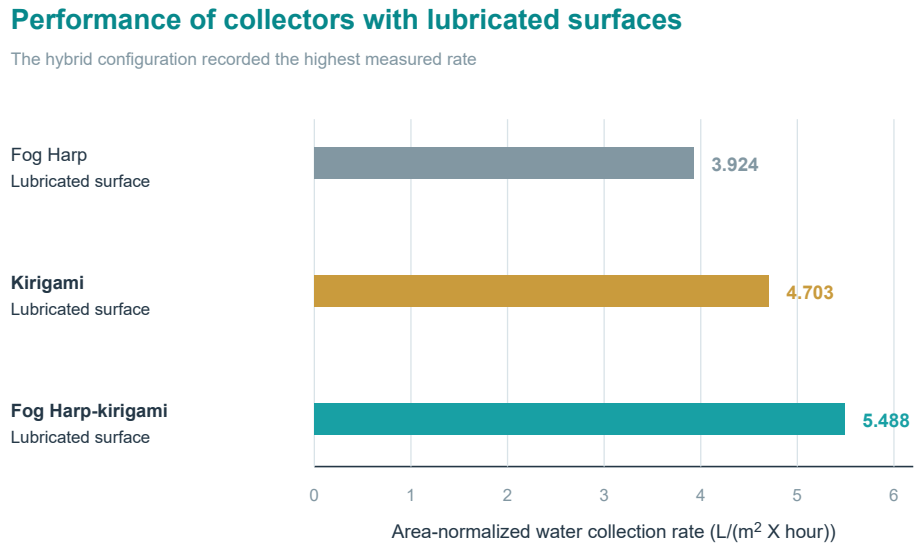


Figure 11 Area-normalized water collection rates of the collector configurations with lubricated surfaces. Exact values are shown at the ends of the bars, and the Fog Harp–kirigami arrangement recorded the highest measured rate.

4.4 Overall Performance Comparison

Across all tested conditions, the Fog Harp–kirigami configuration with lubricated surfaces ranked first, followed by the kirigami and Fog Harp with lubricated surfaces. The superhydrophobic-coated kirigami was the highest-performing coated collector, while the uncoated kirigami was the best-performing baseline geometry. These results identify the Fog Harp–kirigami arrangement with lubricated surfaces as the best-performing configuration among those tested under the laboratory conditions used in this study.

5 Discussion

The amount of liquid reaching the collection tray depended on both collector geometry and surface condition. The difference associated with surface condition varied between collectors, which shows that geometry and surface condition need to be considered together. The hybrid Fog Harp–kirigami configuration with lubricated surfaces achieved the highest area-normalized water collection rate.

5.1 Effect of Collector Geometry

The four uncoated collectors were first compared to examine the effect of geometry. The kirigami collector achieved the highest area-normalized water collection rate at 2.576 $\mathrm{L\,m^{-2}\,h^{-1}}$. The Fog Harp ranked second at 2.032 $\mathrm{L\,m^{-2}\,h^{-1}}$, followed by the fine metal mesh at 1.764 $\mathrm{L\,m^{-2}\,h^{-1}}$. The double-layer Raschel mesh produced the lowest rate at 1.501 $\mathrm{L\,m^{-2}\,h^{-1}}$.

The lower performance of the conventional meshes may be related to their intersecting fibres. Water can collect at fibre intersections, partially block the openings, or remain on the mesh instead of draining directly towards the collection tray. The overlapping layers of the Raschel mesh may also create a more complex path for both the fog-laden airflow and the collected liquid. These effects are consistent with the lower area-normalized collection rate measured for the double-layer Raschel mesh.

The Fog Harp uses parallel vertical wires without horizontal intersections. This geometry provides direct downward drainage paths and may reduce water retention on the collector. Its collection rate was 35.4% higher than that of the double-layer Raschel mesh. However, its measured rate remained lower than that of the kirigami collector.

The kirigami collector contains repeated three-dimensional elements with small internal channels. Its three-dimensional shape may increase interactions between the fog-laden airflow and the collector, while the internal channels provide paths that guide the collected liquid towards the tray. Its rate was 71.6% higher than the rate of the double-layer Raschel mesh. Under the laboratory conditions used in this study, kirigami achieved the best performance among the four uncoated collectors. Figure 12 illustrates the proposed geometric mechanisms that may support this performance.

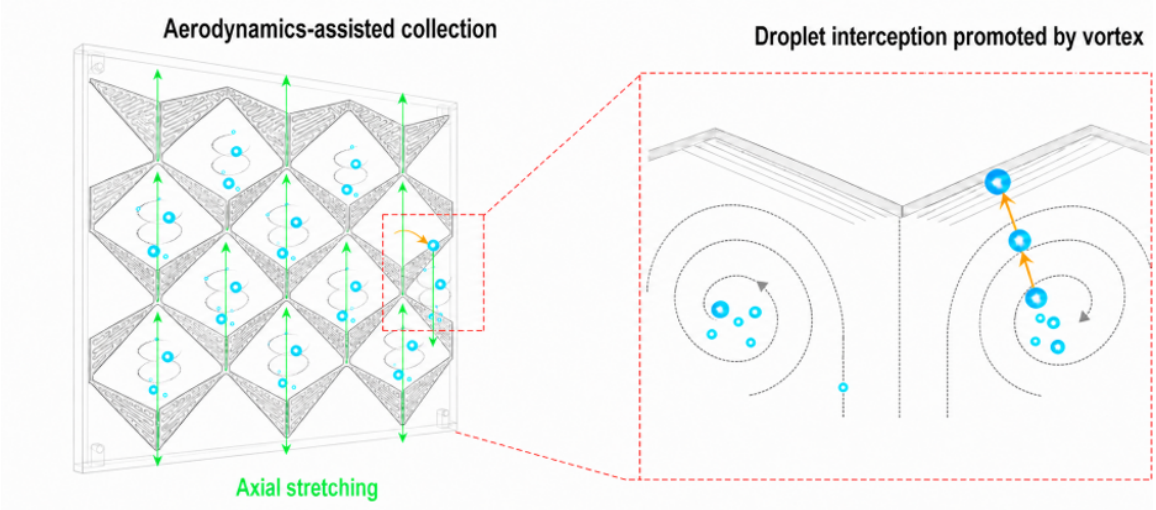


Figure 12 Conceptual interpretation of the collection mechanisms supported by the kirigami geometry. The three-dimensional elements modify the local path of the fog-laden airflow and may promote droplet interception near the folded surfaces. The repeated vertical arrangement and internal channels then provide gravity-directed routes for transporting the collected liquid downward. The enlarged view illustrates how local recirculating flow near a fold may redirect suspended droplets towards the collector surface, consistent with the aerodynamic mechanism reported for three-dimensional kirigami fog collectors [11].

5.2 Effect of Surface Condition

The measured rate differed between surface conditions, and the size of this difference varied between collector geometries. Because some collector dimensions also differed between conditions, these normalized results are treated as condition-level comparisons rather than isolated surface-treatment effects. The superhydrophobic-coated kirigami reached 3.825 $L\,m^{-2}\,h^{-1}$, compared with 2.576 $L\,m^{-2}\,h^{-1}$ for the uncoated kirigami. This rate was 48.5% higher than the uncoated result. The corresponding differences were smaller for the Fog Harp and fine metal mesh, at 9.9% and 8.8%, respectively.

Visible water beading on the coated collectors was consistent with strongly water-repellent behaviour. The reduced contact between the beaded droplets and the underlying surface may have allowed the water to move more easily towards the collection tray. However, the influence of the coating depended on the geometry of the collector, including the orientation of its elements, the presence of intersections, and the available drainage paths. This interaction may help explain why the coated kirigami condition recorded a larger normalized difference than the corresponding Fog Harp and metal-mesh conditions. Representative differences in droplet behaviour under the

three tested surface conditions are shown in Figure 13.

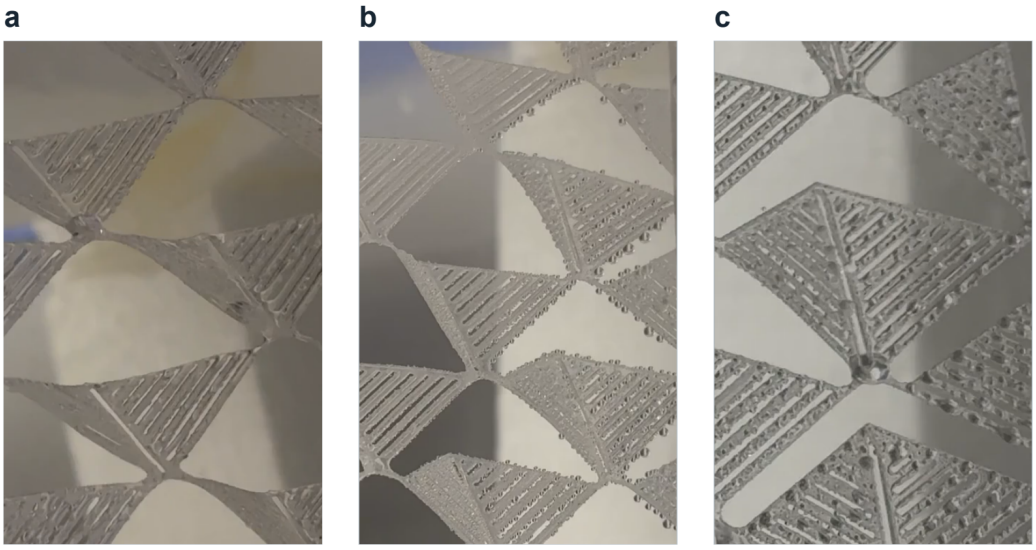


Figure 13 Representative observations of droplet behaviour under the tested surface conditions: (a) uncoated surface, (b) superhydrophobic-coated surface, and (c) lubricated surface. The images qualitatively show differences in droplet shape, visible water beading, and liquid movement across the collector surfaces.

The lubricated condition recorded the highest rate for both collector designs tested under all three surface conditions. The kirigami with a lubricated surface reached 4.703 $L\,m^{-2}\,h^{-1}$. This value was 23.0% higher than that of the superhydrophobic-coated kirigami and 82.6% higher than that of the uncoated kirigami. The Fog Harp with a lubricated surface reached 3.924 $L\,m^{-2}\,h^{-1}$, representing an increase of 75.7% over its superhydrophobic-coated condition and 93.1% over its uncoated condition.

The lubricant may have reduced droplet pinning and promoted easier downward movement of the collected liquid. This effect may have been especially useful for the Fog Harp because its vertical wires already provide direct drainage paths. The observed differences are therefore consistent with an interaction between lubrication, collector geometry, and drainage structure.

5.3 Performance of the Hybrid Collector

The hybrid Fog Harp–kirigami configuration with lubricated surfaces achieved the highest area-normalized water collection rate in the study at 5.488 $L\,m^{-2}\,h^{-1}$. Its rate was 16.7% higher than that of the kirigami with a lubricated surface and 39.9% higher than that of the Fog Harp with a lubricated surface.

In the hybrid arrangement, the Fog Harp was positioned in front of and directly next to the kirigami collector. The fog-laden airflow passed through the Fog Harp before reaching the overlapping part of the kirigami. The Fog Harp may intercept part of the incoming droplets and provide direct vertical drainage paths. At the same time, the downstream kirigami may capture additional droplets and guide the collected liquid through its internal channels towards the shared collection tray. The tested hybrid arrangement is shown in Figure 14.



Figure 14 Hybrid Fog Harp–kirigami configuration during laboratory testing. The Fog Harp wires are positioned in front of the kirigami collector, allowing the fog-laden airflow to pass through both collection structures.

The higher rate achieved by the hybrid configuration is consistent with complementary collection and drainage roles. The Fog Harp provides closely spaced vertical collection elements, while the kirigami introduces a three-dimensional surface with internal drainage channels. Under the tested laboratory conditions, combining these geometries with lubricated surfaces produced the most effective collector configuration examined in this study. The main performance comparisons supporting this discussion are summarised in Table 5.

Table 5 Summary of the main performance comparisons discussed in this study.

Comparison	Reference condition	Increase	Main interpretation
Uncoated Fog Harp	Double-layer Raschel mesh	35.4%	The result is consistent with direct vertical drainage paths without horizontal intersections.
Uncoated kirigami	Double-layer Raschel mesh	71.6%	Three-dimensional elements and internal channels may support droplet collection and liquid drainage.
Superhydrophobic-coated kirigami	Uncoated kirigami	48.5%	Visible water beading and the kirigami drainage geometry were consistent with greater liquid delivery to the tray.
Lubricated kirigami	Uncoated kirigami	82.6%	The lubricated condition was consistent with easier liquid movement through the kirigami channels.
Lubricated Fog Harp	Uncoated Fog Harp	93.1%	The lubricated condition was combined with the direct vertical drainage paths of the Fog Harp.
Hybrid configuration	Lubricated kirigami	16.7%	Combining the Fog Harp and kirigami produced the highest measured collection rate.

6 Limitations and Future Work

6.1 Limitations

This study compared the collectors under controlled laboratory conditions. The results should be interpreted within the following limits:

- The results apply to the collector dimensions, fog source, airflow conditions, and testing periods used in this study.
- Some surface-condition comparisons used collectors with different projected dimensions. Area normalization accounts for frontal area in the reported rate, but dimensional differences may also influence airflow and droplet interception. Therefore, differences between surface conditions cannot be attributed to surface treatment alone.
- The hybrid configuration was normalized using the 80 cm^2 frontal footprint of the larger kirigami collector. Its reported rate represents the performance of the complete Fog Harp–kirigami assembly.
- The measured output represents the liquid that reached the collection tray after interception, coalescence, and drainage.
- One test result was available for each collector and surface condition, so statistical repeatability was not evaluated.
- Most tests used a 30-minute evaluation period, while the superhydrophobic-coated Fog Harp was evaluated for 60 minutes. The same time-normalized equation was applied to all cases.
- Visible water beading was observed on the coated collectors, but quantitative wettability measurements were outside the scope of the experiment.
- The tests examined the initial laboratory performance of the surface treatments rather than their long-term durability or outdoor operation.

6.2 Future Work

Future work should improve repeatability, examine the collection process in more detail, and test the collectors under realistic conditions:

- Repeat every test several times and report the mean collection rate and standard deviation.
- Use the same stabilization and evaluation periods for all configurations.
- Monitor air velocity, relative humidity, fog-water content, and droplet-size distribution.
- Use close-up or high-speed imaging to study droplet interception, coalescence, and drainage.
- Measure contact angle and droplet sliding angle to characterise the coated surfaces quantitatively.
- Test different distances and orientations between the Fog Harp and kirigami collectors.
- Use separate collection trays to study the output of each component in the hybrid configuration.
- Compare different lubricant quantities and grades and examine their performance over repeated tests.
- Conduct long-term outdoor tests in the mountainous regions of southwestern Saudi Arabia.

7 Conclusion

This study examined how collector geometry and surface condition affect passive fog-water collection under controlled laboratory conditions. Four uncoated designs were compared: the kirigami collector, Fog Harp, fine metal mesh, and double-layer Raschel mesh. Kirigami achieved the highest area-normalized water collection rate among the uncoated collectors at 2.576 $\mathrm{L\,m^{-2}\,h^{-1}}$. This result suggests that collector geometry and drainage paths influence how much liquid reaches the collection tray.

Surface treatment was not equally effective for every design. Among the coated conditions, kirigami recorded the largest increase over its uncoated result, while the lubricated conditions recorded the highest rates for both kirigami and Fog Harp. Kirigami with a lubricated surface reached 4.703 $\mathrm{L\,m^{-2}\,h^{-1}}$, and the Fog Harp with a lubricated surface reached 3.924 $\mathrm{L\,m^{-2}\,h^{-1}}$. The effect of a surface treatment therefore depends on how it works with the collector geometry and its drainage structure.

The hybrid Fog Harp–kirigami configuration with lubricated surfaces achieved the highest rate in the study at 5.488 $\mathrm{L\,m^{-2}\,h^{-1}}$. Its performance is consistent with the combination of vertical Fog Harp wires and a three-dimensional kirigami structure with internal drainage channels. Taken together, the results show that collector geometry and surface condition should be designed as parts of one fog-collection system. They also provide a clear basis for repeated laboratory tests and future field evaluation.

References

[1] N. Odnoletkova and T. W. Patzek, "Water Resources in Saudi Arabia: Trends in Rainfall, Water Consumption, and Analysis of Agricultural Water Footprint," *npj Sustainable Agriculture*, vol. 1, art. 7, 2023. doi: https://doi.org/10.1038/s44264-023-00006-w.

[2] A. S. Alzahrani and A. M. Abdelbaki, "Fog Harvesting Implementation as a Sustainable Water Source: A Feasibility Study in Al-Baha, Saudi Arabia," *Journal of Umm Al-Qura University for Engineering and Architecture*, 2025. doi: https://doi.org/10.1007/s43995-025-00250-w.

[3] K. A. Rambo et al., "Water–Energy Nexus in Saudi Arabia," *Energy Procedia*, vol. 105, pp. 3837–3843, 2017. doi: https://doi.org/10.1016/j.egypro.2017.03.782.

[4] P. Gandhidasan and H. I. Abualhamayel, "Exploring Fog Water Harvesting Potential and Quality in the Asir Region, Kingdom of Saudi Arabia," *Pure and Applied Geophysics*, vol. 169, no. 5–6, pp. 1019–1036, 2012. doi: https://doi.org/10.1007/s00024-011-0341-z.

[5] World Meteorological Organization, "Fog," 2017. https://cloudatlas.wmo.int/en/fog.html.

[6] Australian Bureau of Meteorology, "Explainer: What Is Fog?" Aug. 2018. https://media.bom.gov.au/social/blog/1807/explainer-what-is-fog/.

[7] N. Verbrugghe and A. Z. Khan, "Water Harvesting through Fog Collectors: A Review of Conceptual, Experimental and Operational Aspects," *International Journal of Low-Carbon Technologies*, vol. 18, pp. 392–403, 2023. doi: https://doi.org/10.1093/ijlct/ctac129.

[8] M. Damak and K. K. Varanasi, "Electrostatically Driven Fog Collection Using Space Charge Injection," *Science Advances*, vol. 4, no. 6, 2018. doi: https://doi.org/10.1126/sciadv.aao5323.

[9] K.-C. Park et al., "Optimal Design of Permeable Fiber Network Structures for Fog Harvesting," *Langmuir*, vol. 29, no. 43, pp. 13269–13277, 2013. doi: https://doi.org/10.1021/la402409f.

[10] W. Shi et al., "Fog Harvesting with Harps," *ACS Applied Materials & Interfaces*, vol. 10, no. 14, pp. 11979–11986, 2018. doi: https://doi.org/10.1021/acsami.7b17488.

[11] J. Li et al., "Aerodynamics-Assisted, Efficient and Scalable Kirigami Fog Collectors," *Nature Communications*, vol. 12, art. 5484, 2021. doi: https://doi.org/10.1038/s41467-021-25764-4.

[12] D. Seo et al., "The Effects of Surface Wettability on the Fog and Dew Moisture Harvesting Performance on Tubular Surfaces," *Scientific Reports*, vol. 6, art. 24276, 2016. doi: https://doi.org/10.1038/srep24276.

[13] R. S. Schemenauer and P. Cereceda, "A Proposed Standard Fog Collector for Use in High-Elevation Regions," *Journal of Applied Meteorology*, vol. 33, no. 11, pp. 1313–1322, 1994. doi: https://doi.org/10.1175/1520-0450(1994)033<1313:APSFCF>2.0.CO;2.

[14] J. de D. Rivera, "Aerodynamic Collection Efficiency of Fog Water Collectors," *Atmospheric Research*, vol. 102, no. 3, pp. 335–342, 2011. doi: https://doi.org/10.1016/j.atmosres.2011.08.005.

[15] W. Shi et al., "Harps Enable Water Harvesting under Light Fog Conditions," *Advanced Sustainable Systems*, vol. 4, no. 6, art. 2000040, 2020. doi: https://doi.org/10.1002/adsu.202000040.

[16] P.-B. Bintein et al., "Kirigami Fog Nets: How Strips Improve Water Collection," *npj Clean Water*, vol. 6, art. 54, 2023. doi: https://doi.org/10.1038/s41545-023-00266-6.

[17] J. K. Kaindu et al., "Antitangling and Manufacturable Fog Harps for High-Efficiency Water Harvesting," *Droplet*, vol. 2, art. e78, 2023. doi: https://doi.org/10.1002/dro2.78.

[18] Y. Chen et al., "Lubricant Self-Replenishing Slippery Surface with Prolonged Service Life for Fog Harvesting," *Friction*, vol. 10, pp. 1676–1692, 2022. doi: https://doi.org/10.1007/s40544-021-0533-1.

[19] D. M. Fernandez et al., "Fog Water Collection Effectiveness: Mesh Intercomparisons," *Aerosol and Air Quality Research*, vol. 18, no. 1, pp. 270–283, 2018. doi: https://doi.org/10.4209/aaqr.2017.01.0040.

[20] S. Montecinos, D. Carvajal, P. Cereceda, and M. Concha, "Collection Efficiency of Fog Events," *Atmospheric Research*, vol. 209, pp. 163–169, 2018. doi: https://doi.org/10.1016/j.atmosres.2018.04.004.